JOURNAL OF AGRICULTURAL AND FOOD CHEMISTRY
ARTICLE

J. Agric. Food Chem. 2009, 57, 8213–8219 8213
DOI:10.1021/jf9019129

Variations of Water Uptake, Lipid Consumption, and Dynamics during the Germination of *Sesamum indicum* Seed: A Nuclear Magnetic Resonance Spectroscopic Investigation

Bimal Kumar Sarkar,[†] Wei-Yuan Yang,[†] Zhen Wu,[†] Huiru Tang,[‡] and Shangwu Ding*,[†]

[†]Department of Chemistry & Center for Nanoscience and Nanotechnology, National Sun Yat-sen University, 70 Lien-Hai Road, Kaohsiung, Taiwan 80424, Republic of China, and [‡]State Key Laboratory of Magnetic Resonance and Atomic and Molecular Physics, Wuhan Center for Magnetic Resonance, Wuhan Institute of Physics and Mathematics, Chinese Academy of Sciences, Wuhan 430071, People's Republic of China

Germination in sesame seeds (*Sesamum indicum* L.) in water and in indole-3-acetic acid (IAA) solution is investigated with magic-angle-spinning (MAS) solid state nuclear magnetic resonance (NMR) spectroscopy, supplemented by liquid state NMR spectroscopy. The spectra show good resolution and can be assigned with sufficient confidence. The characteristic spectral peaks and relaxation rates were monitored during the entire course of germination for better understanding of the biophysical and biochemical mechanisms involved in the triphasic water uptake of the seed. A highly positive correlation is found between water uptake and lipid consumption during germination. No significant variation is observed in the relaxation times for the lipid protons during the first two stages of triphasic water uptake, while evident differences are observed for water proton relaxation rates in all stages. Although the total amount of water uptake is largely not changed as a result of IAA, the addition of IAA in seed-germination medium has shown some prominent effects on the germination process, e.g, it suppresses lipid consumption and water mobility, and it reduces the longitudinal and transverse relaxation times of lipid protons and causes a more scattered range for these parameters.

KEYWORDS: Germination; sesame seed; nuclear magnetic resonance; relaxation time; water uptake; lipid consumption; indole-3-acetic acid

INTRODUCTION

Dormancy is the general characteristic of all seeds, the degree of which defines what conditions should be satisfied to make the seed germinate (*1*). It also occurs for the seed whose embryo is immature and, in some cases, largely undifferentiated such that further development is needed (*2*). Irrespective of embryo maturity, seeds may be called dormant in the sense that germination is blocked physiologically. Several hypotheses have been proposed to explain the mechanisms of dormancy and the modes of action of dormancy-relieving treatments (*3*−*5*). Under favorable conditions, the quiescent dry seed goes to the nondormant state and germinates as a manifestation of radicle protrusion, i.e., the emergence of the radicle tip through all seed covering layers in association with the elongation of the embryonic axis (*3*). Water uptake plays an important role in the initiation and completion of seed germination. During this process, the dry seed executes triphasic water uptake (*5*), with a quick initial uptake (phase I, i.e., imbibition) followed by a plateau phase (phase II), and a further increase in water uptake (phase III). Also, hormonal changes play a key role in the germination process (*6*). Indole-3-acetic acid (IAA) was proved to be involved in the early stages of germination in Scots pine seedlings (*7*). Not much investigation of IAA activities on the germination of seed has been done so far, which motivated us to explore the possible effects of IAA on the germination of sesame seeds (*Sesamum indicum* L.).

Identification and quantification of the metabolites of a tissue or an organism is fundamentally important for the study of the biology or physiology of, e.g., plants (*8*). To achieve this objective, it is necessary to make use of a range of analytical methods. Mass spectrometry (MS) is a powerful and rather straightforward tool for such types of analysis and is widely used by chemists and biologists, but complementary information from other techniques, particularly nuclear magnetic resonance (NMR) spectroscopy, is invaluable for the identification of plant metabolites. It is well known that the primary plant metabolites are mainly composed of a few elements including hydrogen, carbon, nitrogen, oxygen, phosphorus, and sulfur. All of these elements with the exception of sulfur have magnetic isotopes that can be detected by NMR. Therefore, NMR signals can be used to identify metabolites in plant tissues and their extracts. Also, it is possible to record a series of in vivo spectra from the same sample and then to interpret the metabolic response of the plant material to any change in its physiological state. Simultaneous acquisition of plant metabolism with in vivo ^{1}H NMR spectroscopy and mass spectrometry was first demonstrated in root tissues (*9*). Some

*Corresponding author. Tel: 886-7-525-3917. Fax: 886-7-525-3909. E-mail: ding@faculty.nsysu.edu.tw.

Published on Web 08/24/2009

applications in conjunction with NMR include an analysis of the ligands in barley root exudates (*10*) and a detailed analysis of the composition of tomato fruits (*11*). The metabolite encoded NMR characteristic signals have even led to the detection of new or unexpected compounds (*12*). Furthermore, by using two-dimensional methods, such as heteronuclear single quantum coherence (HSQC), heteronuclear multiple quantum coherence (HMQC), and heteronuclear multiple-bond correlation (HMBC), the detection of some metabolites in plant tissues has been used to analyze anaerobic metabolism in maize root tips (*13*), the composition of barley root exudates (*10*), and nitrogenous metabolites extracted from ^{15}N-labeled *Nicotiana plumbaginifolia* cell suspension cultures (*14*). Besides liquid state NMR spectroscopy, solid state NMR has also been demonstrated to be a powerful tool in the studies of plant metabolism and physiology. For instance, with high resolution MAS NMR, a range of metabolites in the red alga *Gracilariopsis lemaneiformis* (*15*) was unambiguously identified. A particularly interesting methodology demonstrated recently is that the combination of solid state NMR and ^{13}C and ^{15}N isotope labeling can be employed to perform an in vivo study of living plants, as shown by an excellent work which reveals glycine metabolism in intact soybean leaves (*16*). Victor et al. (*17*) reported the detection of free amino acids arginine and asparagine, generated as a result of storage protein mobilization during seed germination and early seedling growth in conifer seeds. They also reported ^{1}H MAS NMR spectra of a single dry seed of western white pine in static state and under moderate MAS speed (3 kHz), and the individual fatty acids were assigned. Furthermore, solid state NMR has even been proved to possess the capacity of identifying specific biochemical reaction mechanisms in a living plant as elegantly demonstrated in a recent work on the role of photorespiration in photosynthesis in intact soybean leaves (*18*).

In this work, the physiological changes occurring in sesame seeds during the germination process are studied based on both solid and liquid state NMR spectra and relaxation dynamics. Emphasis is placed on the changes of water-uptake and oil consumption in the seed and their temporal distribution over different stages of germination. The fatty acids in the sesame seeds during germination were characterized. In addition, to explore the effects of auxin (IAA) on germination, two culture media were used, one being pure water and the other being an aqueous solution of IAA. We found that, with IAA in the culture medium, significant changes in spectral and dynamic characteristics during different stages of germination were observed.

MATERIALS AND METHODS

Seeds and Seed Treatments. Sesame seeds (*Sesamum indicum* L.) were obtained from Kaohsiung, Taiwan. About 10 g of seeds were thoroughly rinsed with water. The seeds were then blotted with filter paper and dried at room temperature (25−30 °C). The dry seeds were stored in sealed plastic bottles at room temperature until they were used. For germination observation, the seeds were placed in water at a constant temperature. Two temperature environments of 25 and 30 °C were tested. At a temperature of 25 °C, it took two days for germination (when shoot appeared) to occur, whereas at 30 °C, the shoot appeared within 12 h. Throughout this work, the results are from germination at temperature 30 °C. Two protocols of germination were applied: sesame seed germination in water and dilute aqueous IAA solution (∼160 ppm). In both environments, the seeds were placed in the solution until the sample was placed into the rotor for NMR measurements. For germination of seeds, an atmosphere with sufficient light and air was maintained. To ensure data reproducibility and perform a reliable error control (for relaxation rates), all experiments were repeated with at least three sets of samples.

Liquid State NMR Spectroscopy. Liquid state NMR (LSNMR) analysis was carried out using a 500 MHz Varian Unity Inova high resolution NMR spectrometer. To prepare samples for traditional liquid state NMR analysis, some seeds were taken from the germination environment (water and IAA solution) at the time scales of 0, 6, 10, and 12 h, blotted, and ground to powder. Normally, 5 grains of seed were used for a single LSNMR experiment. The seed powder was mixed with deuterated chloroform ($CDCl_3$) and tetramethylsilane (TMS) as locking and referencing agents, respectively. ^{1}H NMR spectra were recorded at a resonance frequency of 499.16 MHz with a spectral width of 6 kHz applying a single-pulse sequence with a 5 μs r.f. pulse and a 5 s relaxation delay between scans. Eight scans were accumulated for each ^{1}H NMR spectrum. The assignment of liquid state NMR spectra was assisted by the previously published results of lipids in seeds (*19*−*21*).

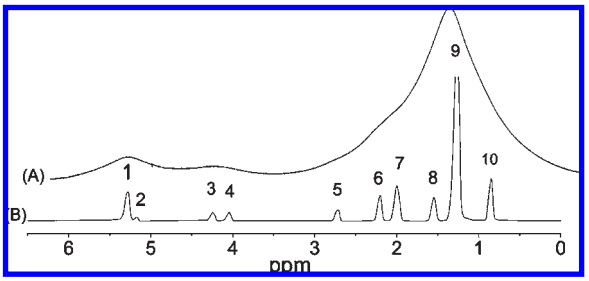

Figure 1. Oil-peak assignment in sesame seeds: (A) static and (B) MAS 1D spectra.

Solid State NMR Spectroscopy. Solid state NMR experiments were performed on a 500 MHz Varian Unity Inova wide bore NMR spectrometer with a MAS control unit, 4 mm (o.d.) rotors. Seeds in different stages of germination were placed in the rotor and spun at a spinning speed of 4 kHz. Normally, 5 grains of seed were used for MAS experiments. ^{1}H MAS NMR spectra were recorded with a spectral width of 15 kHz applying a single pulse (with 90° pulse width of 2.2 μs) and a 5 s relaxation delay between scans. Eight scans were collected for each spectrum. For the longitudinal relaxation measurement, the inversion−recovery method was used with 24 delays. For the transverse relaxation measurement, the CPMG pulse sequence was used with a short 90°−180° interval of 50 μs to minimize the possible slow exchange effect (*22*), although longer intervals up to 200 μs did not show significant differences in transverse relaxation rates.

RESULTS AND DISCUSSION

Assignment of ^{1}H Spectra. Figure 1 shows the one-dimensional (1D) static (A) and MAS (with 4 kHz spinning speed, (B)) ^{1}H spectra of the oil of a single grain of dry sesame seed. For comparison, another spectrum of the mixture of D-chloroform (referenced to 7.28 ppm) and the powder of a dry seed was taken using liquid state NMR (**Figure 2A**). A good agreement was observed between MAS and liquid state NMR spectra. In the second spectrum (lower spectrum), peak X denotes the presence of D-chloroform (i.e., a tiny amount of $CHCl_3$ was generated because of exchange between $CDCl_3$ and residual water in the solvent). Another unexpected peak Y came from an impurity in the D-chloroform solvent. Sesame seed oil is composed of triglycerides (linoleic (18:2), oleic (18:1)) and some saturated fatty acids (*19*). Individual proton resonances are denoted as 1−10 (**Figure 1**). These groups are assigned as (*20*, *21*) (1) $-CH=$, (2) $CHOCO-$, (3) CH_2OCO-, (4) CH_2OCO-, (5) $=CHCH_2CH=$, (6) $-COCH_2-$, (7) $=CHCH_2CH_2$, (8) $-COCH_2CH_2-$, (9) bulk $-CH_2-$, and (10) $-CH_3$. The chemical shifts and relative peak (integral) intensity values are summarized in **Table 1**. For an improved apparent resolution, a part of the liquid state NMR spectrum (from **Figure 2A**) has been magnified as shown in **Figure 2B**. The protons attached to C-2 correspond to the peaks centered at 2.34 ppm, and they are coupled across three bonds to the two nearest neighbors, resulting in the appearance of a typical triplet. The double triplet at 2.09 ppm represents the couplings

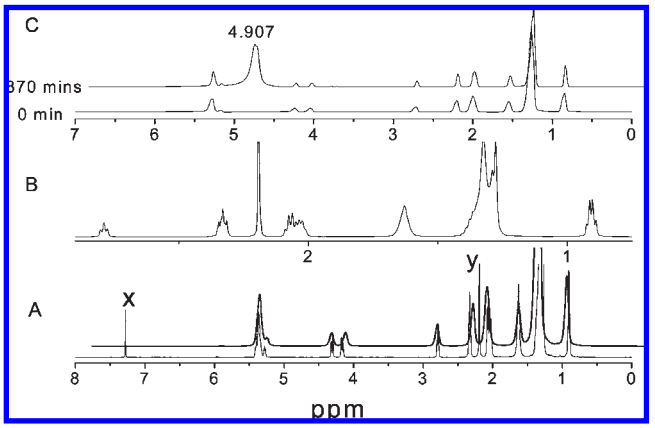

Figure 2. (**A**) ^{1}H peak in MAS (upper spectrum) and LSNMR (lower spectrum, in D-chloroform solution) spectra for dry sesame seeds. A: X, peak from D-chloroform; Y, peak from an impurity in solvent. (**B**) Part of the ^{1}H LSNMR spectrum of dry sesame seeds. (**C**) ^{1}H MAS-spectra at 0 and 870 min. The peak for the water proton (4.907 ppm) has been shown.

Table 1. ^{1}H MAS NMR Resonance Assignment and Spectral Integral Intensity at a MAS Frequency of 4 kHz

peak no. (**Figure 1**)	peak assignment	peak position (ppm)	peak integral intensity	T_1 (s)[a]	T_2 (s)[a]
1	-CH=	5.29	6.83	0.76	0.334
2	CHOCO-	5.19	1.02	0.64	0.334
3	CH_2OCO-	4.27	1.92	0.57	0.071
4	CH_2OCO-	4.06	1.95	0.52	0.072
5	$=CHCH_2CH=$	2.78	2.61	0.67	0.085
6	$-COCH_2$-	2.34	5.82	0.65	0.086
7	$=CHCH_2CH_2$	2.09	8.07	0.53	0.082
8	$-COCH_2CH_2$-	1.57	5.42	0.68	0.085
9	bulk-CH_2-	1.29	41.49	0.68	0.146
10	$-CH_3$	0.91	9.46	1.15	0.327

[a] T_1 and T_2 were measured in intact dry sesame seeds.

with three protons (see **Table 1**). Two protons attached to C-11 in linoleic acid ($=CHCH_2CH=$) can be attributed to the peak at 2.78 ppm. This peak represents two protons found only in linoleic acid. The terminal methyl groups are well distinguished at 0.91 ppm. Two peaks around 5.29 and 5.19 ppm (see **Table 1**) appear from four olefinic protons in linoleic acid and from two olefinic protons in oleic acid, as well as from the CHOCO− group. However, most $-CH_2-$ groups contribute to the peak at 1.29 ppm, and ^{1}H NMR is not sufficient to accurately determine the length of the fatty acid chain.

^{1}H LSNMR and SSNMR Spectra Obtained at Different Germinating Stages. As the first and typical demonstration of the sensitivity of the NMR spectrum to germination, the ^{1}H MAS spectra of a sesame seed germinating in pure water for 0 and 870 min are shown in **Figure 2C**. A pronounced water peak is observed for the spectrum acquired at 870 min. There are other small detectable differences between the two spectra, indicating the change of the distribution of the metabolites. This is further confirmed in **Figure 3** where a series of ^{1}H-LSNMR spectra of sesame seed germinating in pure water at four different times, 0, 360, 600, and 720 min, are shown. Notice that the water peak is at ~1.3 ppm (in D-chloroform solvent). For closer examination, the subspectrum between 3 ppm and 0.5 ppm is shown in the inset. The variations of line shape and number of peaks are clearly shown. This characteristic has been found to be rather general as can be seen from other spectra given below (**Figures 4**−**6**).

Effects of IAA on LSNMR SSNMR Spectra Obtained at Different Germinating Stages. The effects of auxin IAA on sesame

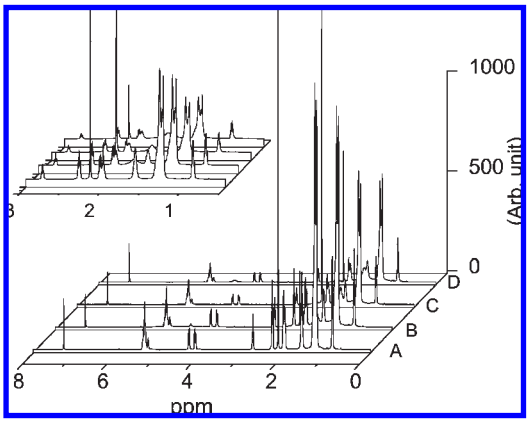

Figure 3. ^{1}H-LSNMR spectra of sesame seed germinating in pure water at (A) 0 min, (B) 360 min, (C) 600 min, and (D) 720 min. Inset: from 3 ppm to 0.5 ppm. Notice that the water peak is at ~1.3 ppm (in D-chloroform solvent).

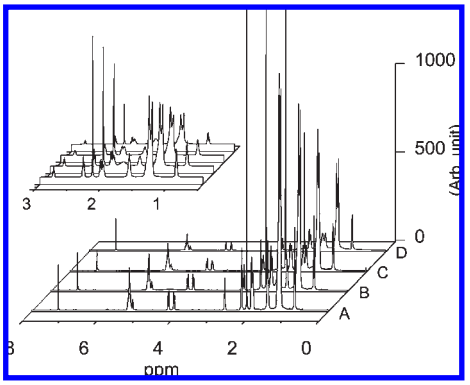

Figure 4. ^{1}H-LSNMR spectra of sesame seed germinating in aqueous IAA solution at (A) 0 min, (B) 360 min, (C) 600 min, and (D) 720 min. Inset: from 3 ppm to 0.5 ppm. Notice that the water peak is at ~1.3 ppm (in D-chloroform solvent).

seed germination can be investigated by comparing the ^{1}H-LSNMR and SSNMR spectra of sesame seed germinating in water and that of sesame seed germinating in aqueous IAA solutions. **Figure 4** shows the ^{1}H-LSNMR spectra of sesame seed germinating in IAA aqueous solution at four different times: 0, 360, 600, and 720 min. Comparing **Figures 3** and **4**, one can notice the clear distinctions between the two groups of spectra, both number of peaks and lineshapes being changed with the addition of IAA. The significant effects of IAA on germination have also been observed from SSNMR spectra as can be seen from **Figure 5** where the ^{1}H MAS spectra of sesame seed germinating in aqueous IAA solution and pure water, acquired at 12 different times are shown. This characteristic becomes more noticeable by comparing the signal intensities of water proton and an oil proton in the two different germination cultures, given in **Figure 6**. Further discussion on the implications of these effects is given in the subsections following the next subsection.

Variations of Relaxation Times and the Effects of IAA on Relaxation at Different Germinating Stages. Analogous to the variations of spectral characteristics over the course of germination, relaxation times of water and lipid protons have been found to vary substantially, indicating that relaxation times (rates) are a sensitive probe to the change of dynamics of the local environment of water and lipids. The effects of auxin IAA on relaxation times are also unambiguously observed. For instance, the transverse relaxation times of the water proton of the sesame seeds

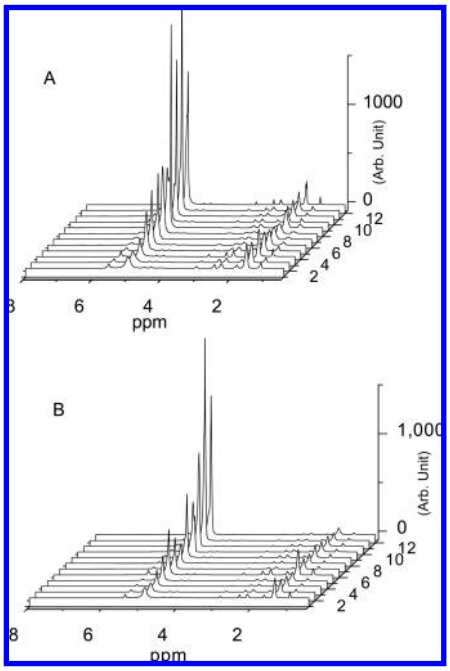

Figure 5. ^{1}H MAS spectra of sesame seed germinating (**A**) in aqueous IAA solution at a 1−12 time scale of 285, 580, 870, 1110, 1755, 2000, 2250, 2530, 2895, 3250, 3450, and 3750 min and (**B**) in pure water at a 1−12 time scale of 285, 580, 870, 1110, 1755, 2000, 2250, 2530, 2895, 3250, 3450, and 3750 min.

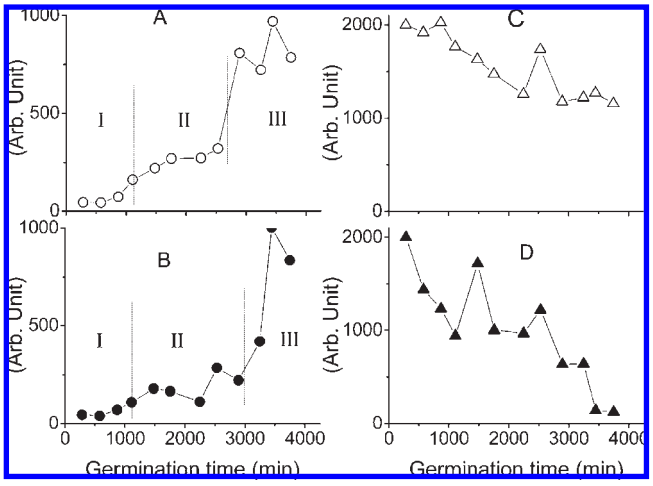

Figure 6. (**A**) Peak integral of the water proton signal taken from **Figure 5A** in aqueous IAA solution. (**B**) Peak integral of the water proton signal taken from **Figure 5B** in pure water. (**C**) Peak integral of the oil proton signal taken from **Figure 5A** in aqueous IAA solution. (**D**) Peak integral of the oil proton signal taken from **Figure 5B** in pure water. For oil proton, signal peaks of the oil are considered.

germinating in two different cultures are shown in **Figure 7**. Similar, but not identical, characteristics have been observed for the longitudinal relaxation times (T_1) as exemplified by the T_1 values of water proton of the sesame seeds germinating in two different cultures, as shown in **Figure 8**. As anticipated, the relaxation times of lipid protons also vary significantly, although differently from that of the water proton, as demonstrated in **Figure 9** where the transverse relaxation times of lipid protons at different geminating times are plotted. The implications of these observations are discussed below.

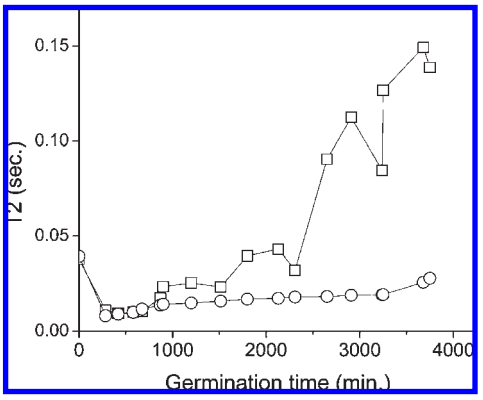

Figure 7. Temporal T_2 variation of water-proton during seed germination in pure water (□) and aqueous IAA solution (○). The size of the symbols showing the data points in the diagram gives an indication of the experimental errors.

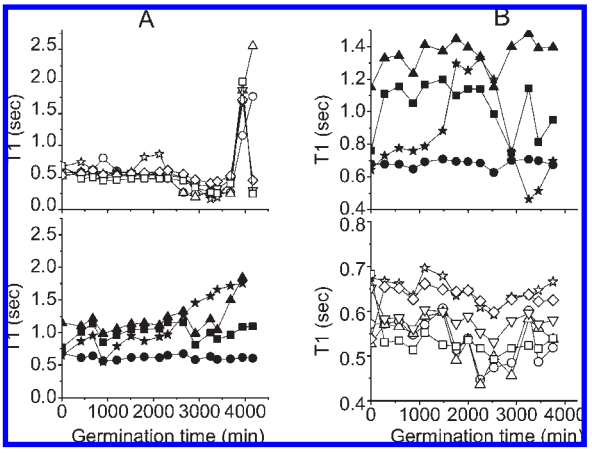

Figure 8. Temporal variation of T_1 for proton in different peaks; ■, peak 1; ★, peak 2; ○, peak 3; △, peak 4; ☆, peak 5; ▽, peak 6; ◇, peak 7; □, peak 8; ●, peak 9, ▲, peak 10, during germination (**A**) in pure water and (**B**) in aqueous IAA solution (see peak no. in **Table 1**). The size of the symbols showing the data points in the diagram gives an indication of the experimental errors.

In the following subsections, the biophysical and functional implications of the above observations on sesame seeds at different germination times and germinating in different cultures are discussed, highlighting the variations of structure and local dynamics of water and lipids as well as the effects of auxin. It is also hoped that the feasibility and unique advantages of applying NMR to the investigation of intact seeds is demonstrated in the context.

Water Uptake and Lipid Consumption during Germination. ^{1}H MAS spectra of an intact sesame seed after it was placed in a water environment for germination for 0 and 870 min are shown in **Figure 2C**. A strong peak of water proton appears at 4.907 ppm at 870 min, showing that the seed has a permeable coat in the water absorption process. For a better understanding of water uptake and the change in metabolites of the sesame seed in the germination process, in addition to MAS ^{1}H spectra, liquid state NMR spectra of sesame seeds germinating in different culture media (pure water and IAA aqueous solution) were also obtained at different times of germination as shown in **Figures 3** and **4**. Shown in **Figure 3** are the liquid state NMR spectra recorded for the germinating seed in a pure water environment at 0, 360, 600, and 720 min. Except for the water peak at ∼1.3 ppm (because the

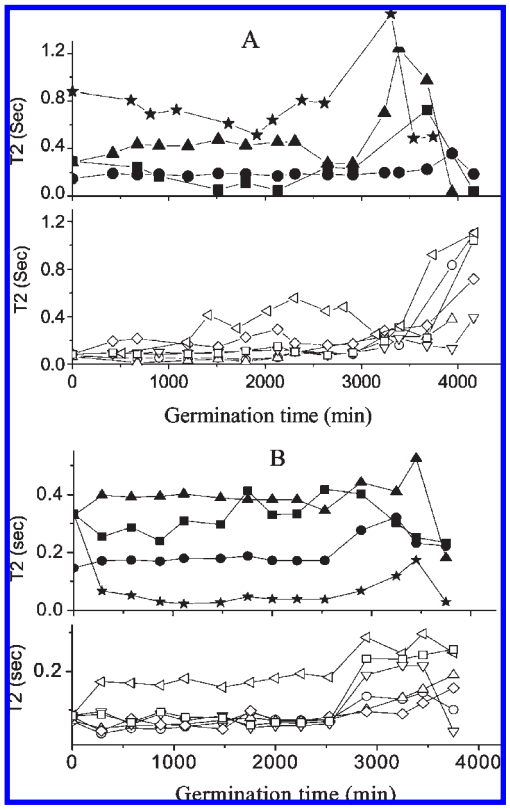

Figure 9. Temporal variation of T_2 for proton in different peaks; ■, peak 1; ★, peak 2; ○, peak 3; △, peak 4; left-pointing triangle, peak 5; ▽, peak 6; ◇, peak 7; □, peak 8; ●, peak 9, ▲, peak 10, during germination (**A**) in pure water and (**B**) in aqueous IAA solution (see peak no. in **Table 1**). The size of the symbols showing the data points in the diagram gives an indication of the experimental errors.

solvent used was D-chloroform), the resonance peaks are the same as those in **Figure 2**. **Figure 4** shows the liquid state NMR resonance peaks at the time scales of 0, 360, 600, and 720 min on the germination of the seed in aqueous IAA solution. From **Figures 3** and **4**, oil consumption is clearly seen because the intensities of all oil peaks uniformly decrease as germination proceeds. At the end of phase I, less than 20% of oil is left. The difference between **Figures 3** and **4** lies mainly in the intensities rather than the number of peaks, chemical shifts, or line shape, indicating that the addition of IAA changes the germination rate but does not change the composition of metabolites. However, increase of water uptake is not clearly shown in both **Figures 3** and **4**. We attribute this to the overlap of the water peak and CH_2 peak (which decreases with germination time), and the exchange of water and D-chloroform. This also shows that liquid state NMR spectroscopy alone is not sufficient for quantitative studies of seed germination. By contrast, a remarkable change in the water proton signal intensity is observed in the ^{1}H MAS spectra (**Figure 5A**,**B**) taken at different times of germination of the seed (from 285 up to 3750 min) in aqueous IAA solution and pure water environments, respectively. The peak centered at ~4.9 ppm in the MAS spectrum, which has been assigned to the hydration water in the seed, grows in intensity and decreases in line width as water uptake proceeds. This line narrowing reflects the increasing mobility of the water molecules as hydration sites on macromolecules are filled, characterized as loosely bound water in the initial stage and as increasingly free water. Though free and bound water molecules have not been distinctly differentiated in a universal context (*22*), it is reasonable to infer that bound water is restricted in motion and associated to some extent with hydration sites on macromolecules, whereas free water has properties more like those of pure liquid-state water.

Solid state NMR spectra such as in **Figure 5A** and **B** can be used for quantitative analysis because there is no proton exchange between water and solvent, and there is no spectral overlap between water and other compounds. The changes in the water proton signal intensity in the germination metabolism in the aqueous IAA solution and water environments are elaborately demonstrated in **Figure 6A** and **B**, respectively. The water ingression into the seed is a common feature as revealed in both figures. Various hydrophilic groups ($-NH_3$, $-OH$, and/or $-COOH$) of proteins and carbohydrates located in the seed coat attract dipolar molecules of water to form a hydrated shell around the macromolecules, which facilitates the imbibitional force and results in swelling of the seed. The germinating seed, therefore, exhibits an increase in relative water content with the lapse of time. The temporal variation of the water proton signal intensity exhibits a three-stage water uptake process, consisting of imbibition (stage I), activation, or germination (stage II), and growth (stage III). Though there is a difference in the time of occurrence of the stages in the two environments of germination, the trend is alike, following the three-stage model of germination metabolism (*5*). In the imbibition stage, the process of water absorption reactivates enzymes present in the seed. These enzymes break down storage compounds in the seed to make them available for the next germination stage of a typical plateau phase II. A further increase in water uptake (phase III) occurs only when germination is completed, as the embryo axis elongates and breaks through its covering structures (*5*). For the completion of radicle protrusion, cell elongation is necessary and is generally accepted to be sufficient for the emerging radicle to start to grow (*23*), indicating that cell divisions may not be required for radical protrusion (*24*). It can be anticipated that the temporal variation of each stage should depend on properties inherent to the seeds such as the testa permeability and seed size as well as external conditions such as temperature, oxygen level, light, etc. In the commencement of phase III, the high matrix potential of the seed increases the water potential difference between the seed and the substrate, resulting in rapid water uptake (*25*).

Moreover, the lipid consumption profile can also been obtained from **Figure 5**. Shown in **Figure 6C** and **D** are the lipid signals at different germination times and in different germination media. A highly positive correlation between water uptake and lipid consumption is revealed by comparing **Figure 6A** to **C** and **B** to **D**, repectively. It is also clear that while water uptake is largely the same for both culture media, lipid consumption is faster with pure water as culture medium than that with IAA solution as culture medium. It seems to indicate that lipid consumption is suppressed by IAA.

Variation of Dynamics during Germination. Dynamics of water and lipids during the entire course of germination can also be systematically investigated with relaxation times. The spin−spin relaxation times (T_2) of water proton at different germination times in pure water as well as IAA medium are shown in **Figure 7**. Three stages of water uptake in the seed are reflected in the variation of T_2 of the water proton in the pure water medium, whereas no significant variation in T_2 has been observed in the IAA medium. In the first stage, the T_2 variation is more or less flat, indicating that the water molecules are in slow motion during imbibition as the correlation times for the motion of bound water and macromolecules are most likely too long because most of the seed components are relatively rigid. This steady-state value of T_2 can be ascribed to water imbibition through the seed coat. The seed coat imposes a physical constraint to radicle protrusion,

which has to be overcome by the growth potential of the embryo in the second phase. In nonendospermic seeds, the cell layer of the testa is mainly responsible for this coat dormancy (*26*). In many mature nonendospermic seeds, complete endosperm assimilation occurs during seed development, and the embryo is enclosed by the testa as the only covering layer. In the second stage, T_2 increases slowly with nonuniform rates, becoming steeper in the later part (stage III). Here, it can be noted that the water proton relaxes with decreasing correlation time while water uptake follows a plateau phase, which supports the fact that the increase in the relaxation time may be described as the result of higher mobility of water through the processes of rupture of the testa and the endosperm, two distinct and temporally separate events during germination (*27*). A typical visible distinction between testa and endosperm rupture has been observed for the seed germination of the Cestroideae (*Nicotiana*, *Petunia*) subgroup of the Solanaceae (*28*). This distinction is seen from the T_2 changes during the second phase (with water as medium). T_2 increases more rapidly at the end of the second phase. It means that in postgermination (stage III) of the embryo, water uptake is the fastest as a result of metabolic pull in the synthesis of proteins and enzymes. Also, hormones play important roles in these pathways (*29*). The primary actions of hormones include the promotion of radial cell expansion in the embryonic hypocotyl, enhancement of seed respiration, and water potential, which in turn may increase the relaxation time of the water proton. However, the triphasic variation of T_2 of the water proton is much less pronounced in the IAA medium. This means that although IAA does not affect the total water uptake it does affect water mobility. The fact that IAA suppresses lipid consumption and water mobility signifies a substantial modification of the metabolism pathways in the germination with the addition of IAA. This is an interesting observation but not a surprising one. The role for auxins in apical−basal pattern formation during embryogenesis (*30*) has been found, but very little is known at the molecular level about the role of auxin during seed germination. Free IAA has been reported to decrease during the imbibition of Sorghum grains (*31*). It has also been found that catalase expression in the scutellum of germinating maize kernels is regulated by auxin (*32*). Moreover, an IAA-modified protein from bean seeds, lAP1, which is a distinct class of conjugated phytohormones as a major form of auxin, has been identified to be associated with rapid growth during seed development (*33*). It is worth noting that the postgermination accumulation of ACO (1-aminocyclopropane-1-carboxylic acid oxidase), the ethylene-forming enzyme, and the ethylene production of chick-pea seedlings are promoted by IAA (*34*).

Variations in T_1 and T_2 for oil proton groups are also worth investigating. The values of T_1 and T_2 for each group in a dry seed are given in **Table 1**. They reflect differences in proton−proton distances and segmental mobility. The short relaxation times of CH_2 groups can be attributed to the efficient relaxation mechanism due to mutual magnetic dipole−dipole interactions among the neighboring proton pairs. The central part of the molecule is more rigid, leading to values of $T_1 < 0.68$ s and $T_2 < 0.09$ s. However, the segmental mobility increases along the fatty acid chain and causes less effective relaxation times of $T_1 = 0.68$ s and $T_2 = 0.15$ s for the bulk CH_2 group (oscillating around 1.29 ppm). The terminal methyl protons have the longest relaxation time, indicating that methyl protons rotate even faster, whereas CH protons are not relaxed as quickly because they interact only with remote partners. Also the values of $T_1 = 0.76$ and 0.64 s for −CH═ groups in the chain reveal that they undergo faster motion than the glyceride proton CHOCO− in the central part of the molecule. However, looking at the temporal variation in relaxation times of the oil protons, we do not see a clear triple-phase pattern. Unlike water proton relaxation, there is no prominent variation in the T_1 values of oil protons during the first two stages of water uptake as shown in **Figure 8A** and **B**. The bound protons can efficiently exchange polarization with both starch and protein protons. To a large extent, this spin-exchange process averages out T_1 differences among starch, protein, and water protons. Proton spin−lattice relaxation within the seed may proceed over a range of rates centered at around the average rate observed. The relaxation rates for oil peaks on the central part of the molecule (at 1.57, 2.09, 2.34, 2.78, 4.06, and 4.27 ppm) have similar values without any appreciable variation during the imbibition and germination processes. But the other terminal peaks (at 0.91, 1.29, 5.19, and 5.29 ppm) have the larger value of T_1, indicating that their dynamicity is much greater than that of the central part of the oil molecule. Also, a peculiar behavior regarding the variation in T_1 values of the central part has been observed in the pure water germination environment. There is an up-rising tendency of T_1 values in the final stage of water uptake. But this kind of behavior is not observed in the aqueous IAA environment (**Figure 8B**), which confirms that the IAA medium creates a different atmosphere of metabolism in germination. However, by comparing **Figure 8A** with **B**, it is clear that IAA reduces the longitudinal relaxation times of almost all lipid protons and causes a much more scattered distribution of them.

An analogous trend of temporal variation is observed in spin−spin relaxation times (T_2) of the oil protons in a water germinating environment (**Figure 9A**). The oil proton T_2 values do not vary markedly in the first two stages. The bulk methylene protons at 1.29 ppm manifest a T_2 value of ∼19 ms in both germination media, corresponding to a fairly mobile regime. The T_2 values of these protons do not change throughout imbibition. For solids, T_2 values are typically determined by dipolar couplings and are rather short. For example, the transverse proton magnetization in a rigid $-(CH_2)_n-$ chain dephases rapidly, with a time constant as small as $10^{-6}-10^{-5}$ s. However, if the $-(CH_2)_n-$ chain is in rapid motion, as in the case of the lipid membrane chain in the seed, the dipolar couplings between protons are not so strong, resulting in slower magnetization dephasing of lipid protons, i.e., larger proton T_2 values. Therefore, we may infer that the lipid structure is in a semisolid-like phase. Again, as expected, T_2 values for all lipid protons have an up-rising tendency in the postgermination stage of the seed in a water environment. But the up-rising tendency of T_2 is not so prominent in the postgermination occurring in an IAA environment (**Figure 9B**). It is also easy to find that with IAA, the T_2 values of almost all lipid protons are reduced and are scattered in a much broader range. A straightforward explanation for these phenomena is that IAA blocks the accessibility of water molecules to oil molecules, but the definite answer to the question of why this happens has to be left for further investigations. It is certainly related to the biological activities involving water and oil as well as auxin, such as metabolism and enzymatic reactions in the postgermination stage. For instance, auxin has been found to play a positive role in the increase of the permeability of the membrane for the diffusing water (*35*). Moreover, hydration of the seed is also associated with the activation of the existing proteins and synthesis of a specific hydrolytic enzyme. The level of such proteins is determined by various hormones including auxins (*36*). Again, the activity of the enzyme not only depends on the presence of substrate but also on some other external and internal factors. One such factor is the level of phytohormones. If the auxin concentration in the seeds increases, enzymatic activities are elevated (*37*). This may be the consequence of the suppressive action of auxin to a specific gene, to activate transcription and

translation (*35*). We believe that a satisfactory explanation of our observations will help us in forming a better understanding of its developmental physiology.

ABBREVIATIONS USED

NMR, nuclear magnetic resonance; MAS, magic angle spinning; IAA, indole-3-acetic acid; HSQC, heteronuclear single quantum coherence; HMQC, heteronuclear multiple quantum coherence; HMBC, heteronuclear multiple-bond coherence.

LITERATURE CITED

(1) Bradford, K. J. Population-Based Models Describing Seed Dormancy Behavior: Implications for Experimental Design and Interpretation. In *Plant Dormancy: Physiology, Biochemistry and Molecular Biology*; Lang, G. A., Ed.; CABI: Wallingford, U.K., 1996; pp 313−339.

(2) Baskin, C. C.; Baskin, J. M. *Seeds: Ecology, Biogeography and Evolution of Dormancy and Germinaton*; Academic Press: San Diego, CA, 1998; p 666.

(3) Bewley, J. D.; Black M. *Seeds: Physiology of Development and Germination*; Plenum Press: New York, 1994; p 445.

(4) Foley, M. Carbohydrate Metabolism As a Physiological Regulator of Seed Dormancy. In *Plant Dormancy: Physiology, Biochemistry and Molecular Biology*, Lang, G. A., Ed.; CABI: Wallingford, U.K., 1996; pp 245−256.

(5) Bewley, J. D. Seed germination and dormancy. *Plant Cell* **1997**, *9*, 1055–1066.

(6) Ross, J.; O'Neill, D. New interactions between classical plant hormones. *Trends Plant Sci*. **2001**, *6*, 2–4.

(7) Ljung, K.; Ostin, A.; Lioussanne, L.; Sandberg, G. Developmental regulation of indole-3-acetic acid turnover in Scots pine seedlings. *Plant Physiol*. **2001**, *125*, 464–475.

(8) Sumner, L. W.; Mendes, P.; Dixon, R. A. Plant metabolomics: large-scale phytochemistry in the functional genomics era. *Phytochemistry* (*Elsevier*) **2003**, *62*, 817–836.

(9) Fan, T. W.-M.; Higashi, R. M.; Lane, A. N.; Jardetzky, O. Combined use of 1H NMRand GC-MS for metabolite monitoring and in vivo 1H NMR assignments. *Biochim. Biophys. Acta* **1986**, *882*, 154–167.

(10) Fan, T. W.-M.; Lane, A. N.; Pedler, J.; Crowley, D.; Higashi, R. M. Comprehensive analysis of organic ligands in whole root exudates using nuclear magnetic resonance and gas chromatography-mass spe ctrometry. *Anal. Biochem*. **1997**, *251*, 57–68.

(11) Noteborn, H. P. J. M.; Lomnmen, A.; Van der Jagt, R. C.; Weseman, J. M. Chemical fingerprinting for the evaluation of unintended secondary metabolic changes in transgenic food crops. *J. Biotechnol*. **2000**, *77*, 103–114.

(12) Gout, E.; Aubert, S.; Bligny, R.; Rébeillé, F.; Nonomura, A. R.; Benson, A. A.; Douce, R. Metabolism of methanol in plant cells: Carbon-13 nuclear magnetic resonance studies. *Plant Physiol*. **2000**, *123*, 287–296.

(13) Shachar-Hill, Y.; Pfeffer, P. E.; Gerrnann, M. W. Following plant metabolism in vivo and in extracts with heteronuclear two-dimensional nuclear magnetic resonance spectroscopy. *Anal. Biochem*. **1996**, *243*, 110–118.

(14) Mesnard, F.; Azaroual, N.; Marty, D.; Fliniaux, M.-A.; Robins, R. J. Use of 15N reverse gradient two-dimensional nuclear magnetic resonance spectroscopy to follow metabolic activity in *Nicotiana plumbaginifolia* cell suspension cultures. *Planta* **2000**, *210*, 446–453.

(15) Broberg, A.; Kenne, L.; Pedersen, M. In situ identification of major metabolites in the red alga *Gracifariopsis lemnaneiformis* using high resolution magic angle spinning magnetic resonance spectroscopy. *Planta* **1998**, *206*, 300–307.

(16) Cegelski, L.; Schaefer, J. Glycine metabolism in intact leaves by in vivo ^{13}C and ^{15}N labeling. *J. Biol. Chem*. **2005**, *280*, 39238–39245.

(17) Victor, V.; Terskikh, J.; Feurtado, A.; Borchardt, S.; Giblin, M.; Abrams, S. R.; Kermodel, A. R. In vivo ^{13}C NMR metabolite profiling: potential for understanding and assessing conifer seed quality. *J. Exp. Bot*. **2005**, *56*, 2253–2265.

(18) Cegelski, L.; Schaefer, J. NMR determination of photorespiration in intact leaves using in vivo $^{13}CO_2$ labeling. *J. Magn. Reson*. **2006**, *178*, 1–10.

(19) Sengupta, A.; Roychoudhury, S. K. Triglyceride composition of *Sesamum indicum* seed oil. *J. Sci. Food Agric*. **1976**, *27*, 165–169.

(20) Sacchi, R.; Medina, T.; Aubourg, S. P.; Addeo, F.; Palillo, L. Proton nuclear magnetic resonance rapid and structure-specific determination of ω-3 polyunsaturated fatty acids in fish lipids. *J. Am. Oil Chem. Soc*. **1993**, *70*, 225–228.

(21) Wanasundara, U. N.; Shahidi, F. Application of NMR spectroscopy to assess oxidative stability of canola and soybean oils. *J. Food Lipids* **1993**, *1*, 15–24.

(22) Kuntz, I. D.; Kauzmann, W. Hydration of proteins and polypeptides. *Adv. Protein Chem*. **1974**, *28*, 239–345.

(23) Barroco, R. M.; Van Poucke, K.; Bergervoet, J. H. W.; De Veylder, L.; Groot, S. P. C.; Inze, D.; Engler, G. The role of the cell cycle machinery in resumption of postembryonic development. *Plant Physiol*. **2005**, *137*, 127–140.

(24) Bewley, J. D.; Black, M. *Physiology and Biochemistry of Seeds*; Springer Verlag: New York, 1978; Vol. *1*, p 306.

(25) Leopold, A. C. Volumetric components of seed imbibition. *Plant Physiol*. **1983**, *73*, 677–680.

(26) Debeaujon, I.; Le′on-Kloosterziel, K. M.; Koornneef, M. Influence of the testa on seed dormancy, germination, and longevity in *Arabidopsis*. *Plant Physiol*. **2000**, *122*, 403–413.

(27) Leubner-Metzger, G. Functions and regulation of β-1,3-glucanase during seed germination, dormancy release and after-ripening. *Seed Sci. Res*. **2003**, *13*, 17–34.

(28) Krock, B.; Schmidt, S.; Hertweck, C.; Baldwin, I. T. Vegetation-derived abscisic acid and four terpenes enforce dormancy in seeds of the post-fire annual, *Nicotiana attenuata*. *Seed Sci. Res*. **2002**, *12*, 239–252.

(29) Kepczynski, J.; Kepczynska, E. Ethylene in seed dormancy and germination. *Physiol. Plant*. **1997**, *101*, 720–726.

(30) Teale, W. D.; Paponov, I. A.; Ditengou, F.; Palme, K. Auxin and the developing root of *Arabidopsis thaliana*. *Physiol. Plant*. **2005**, *123*, 130–138.

(31) Dewar, J.; Taylor, J. R. N.; Berjak, P. Changes in selected plant growth regulators during germination in sorghum. *Seed Sci. Res*. **1998**, *8*, 1–8.

(32) Guan, L. Q. M.; Scandalios, J. G. Catalase gene expression in response to auxin-mediated developmental signals. *Physiol. Plant*. **2002**, *114*, 288–295.

(33) Walz, A.; Park, S.; Slovin, J. P.; Ludwig-Muller, J.; Momonoki, Y. S.; Cohen, J. D. A gene encoding a protein modified by the phytohormone indoleacetic acid. *Proc. Natl. Acad. Sci. U.S.A*. **2002**, *99*, 1718–1723.

(34) Go′mez-Jime′nez, M. C.; Garcia-Olivares, E.; Matilla, A. J. 1-Aminocyclopropane-1-carboxylate oxidase from embryonic axes of germinating chick-pea (*Cicer arietinum* L.) seeds: cellular immunolocalization and alterations in its expression by indole-3-acetic acid, abscisic acid and spermine. *Seed Sci. Res*. **2001**, *11*, 243–253.

(35) Hopkings, W. G. *Introduction to Plant Physiology*; John Wiley and Sons, Inc.: New York, 1995.

(36) Hirasawa, E. Auxins induce α-amylase activity in pea cotyledons. *Plant Physiol*. **1989**, *91*, 484–486.

(37) Ahmad, A. Hayat, S. Response of Nitrate Reductase to Substituted IAA in Pea Seedlings. In *Plant Physiology for Sustainable Agriculture*; Srivastava, G. C., Singh, K., Pal, M., Eds.; Pointer Publisher, Jaipur, India, 1999; pp 252−259.

Received June 4, 2009. Revised manuscript received July 31, 2009. Accepted August 06, 2009. This work was supported by the Program for Promoting Academic Excellence of Universities funded by the National Science Council of the Republic of China (S.D., Contract Nos. NSC-96-2752-M-110-001-PAE and NSC-97-2752-M-110-001-PAE).